## SUPPLEMENTARY MATERIALS AND METHODS

*Complementation mutator assay*

Cells lacking a functional chromosomal *mutS* gene show a mutator phenotype, which is analyzed by the frequency of rifampicin-resistant clones arising from unrepaired polymerase errors in the *rpoB* gene (60). Single colonies of *mutS* deficient TX2929 cells transformed with vector control or plasmids carrying the indicated gene were grown overnight at 37°C in 3 ml LB cultures containing 100 μg/ml ampicillin. Five independent single colonies were used per plasmid. Aliquots of 50 μl of the undiluted or $10^{-6}$ diluted culture were plated on LB-agar plates containing 25 μg/mL ampicillin with or without 100 μg/mL rifampicin. Colonies were counted after o/n incubation at 37°C.

*In vitro DNA mismatch repair activity assay*

DNA mismatch repair activity was assessed by MutH activation. For this assay, $His_6$-tagged MutS, MutL and MutH were expressed and purified as described (61). 400 nM MutS, 1 μM MutL and 200 nM MutH were used to cleave 10 nM of G·T-mismatch containing DNA of 484 base pairs (generated as described (62)) in 10 mM Tris-HCl pH 7.9, 5 mM $MgCl_2$, 1 mM ATP, 50 μg/ml BSA and 125 mM KCl at 37°C for 1 to 30 min. MutH endonuclease activity was scored by the appearance of cleaved products and analyzed by 6% PAAG electrophoresis.

*Fluorescence polarization (FP) competition assay*

FP measurements were done *in duplo* at room temperature, in a 96-well plate with 50 μl of sample per well in buffer (25 mM Hepes pH 7.5, 150 mM KCl, 5 mM $MgCl_2$, 0.05% TWEEN-20). Each sample contained 0.5 nM of TAMRA-labeled 21-bp DNA with a G·T mismatch (same 21-bp sequence as in the SAXS experiments) and 32 nM of MutS D835R. Competition was assessed by presence of increasing concentrations of unlabeled DNA with the same sequence; either 21-bp duplex or 21-bp duplex with a $(dT)_{20}$ ssDNA overhang. After 10 minutes of equilibration at room temperature, FP was measured using a PheraStar Plate Reader (BMG Inc.).

*Electrophoretic mobility shift assay*

A radioactively labeled 41-bp DNA duplex containing a mismatch was obtained as follows. Strand A (ATAGGACGCTGACACTGGTGCTTGGCAGCTTCTAATTCGAT) was incubated with [γ -$^{32}$P]-ATP and T4 PNK enzyme (New England BioLabs) in T4 PNK buffer for 40 minutes at 37 °C. The T4 PNK was subsequently inactivated by boiling the sample for 20 minutes. The labeled strand was then annealed with strand B (ATCGAATTAGAAGCTGCCAGGCACCAGTGTCAGCGTCCTAT) by combining the two strands in a 4:5 ratio in annealing buffer (25 mM Hepes pH 7.5, 150 mM KCl, 10 mM $MgCl_2$) and incubating them together for 20 minutes at 90 °C. The sample was then slowly cooled to room temperature. Excess [γ -$^{32}$P]-ATP was removed from the labeled DNA using a G50 spin column (GE).

1 nM of $^{32}$P-labeled DNA was incubated with varying concentrations of MutS protein (wild type, D835R mutant or cross-linked tetramer) in buffer (25 mM Hepes pH 7.5, 125 mM KCl, 50 μg/mL BSA, 0.5 mM ADP) in a total volume of 20 μL for 15 minutes. 4 μL of loading buffer (50% glycerol, 20 mM EDTA) was then added to the samples. 10 μL of each sample was loaded on a 4% acrylamide gel in TAE buffer and run for 1.5 h at 60 V at 4 °C. The gel was subsequently dried for 1 h and exposed to a phospho-imager plate for 18 h, after which the plate was scanned in a FLA-3000 phospho-imager scanner (Fujifilm).

## SUPPLEMENTARY FIGURES

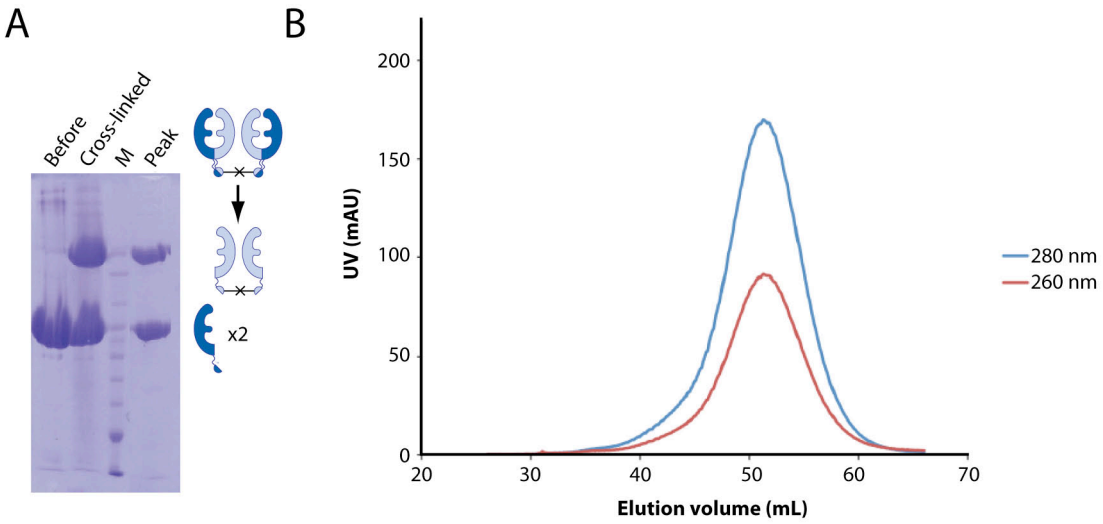


*Supplementary Figure 1.* Formation of obligate MutS tetramers by cross-linking of the single-cysteine MutS R848C with 1,11-bis-maleimido-triethyleneglycol. (A) After cross-linking, two bands can be observed with SDS-PAGE analysis (protein is visualized with coomassie staining), corresponding to a tetramer in which C-terminal domains of two dimers are irreversibly coupled (see schematic representation next to the gel). (B) The stable tetramer runs as a single peak in size-exclusion chromatography (Superdex 200 16/60 column). The slight shoulder at lower elution volume, corresponding to higher-molecular weight molecules, results from a small amount of nonspecific cross-links and was not taken with the rest of the peak for further experiments.

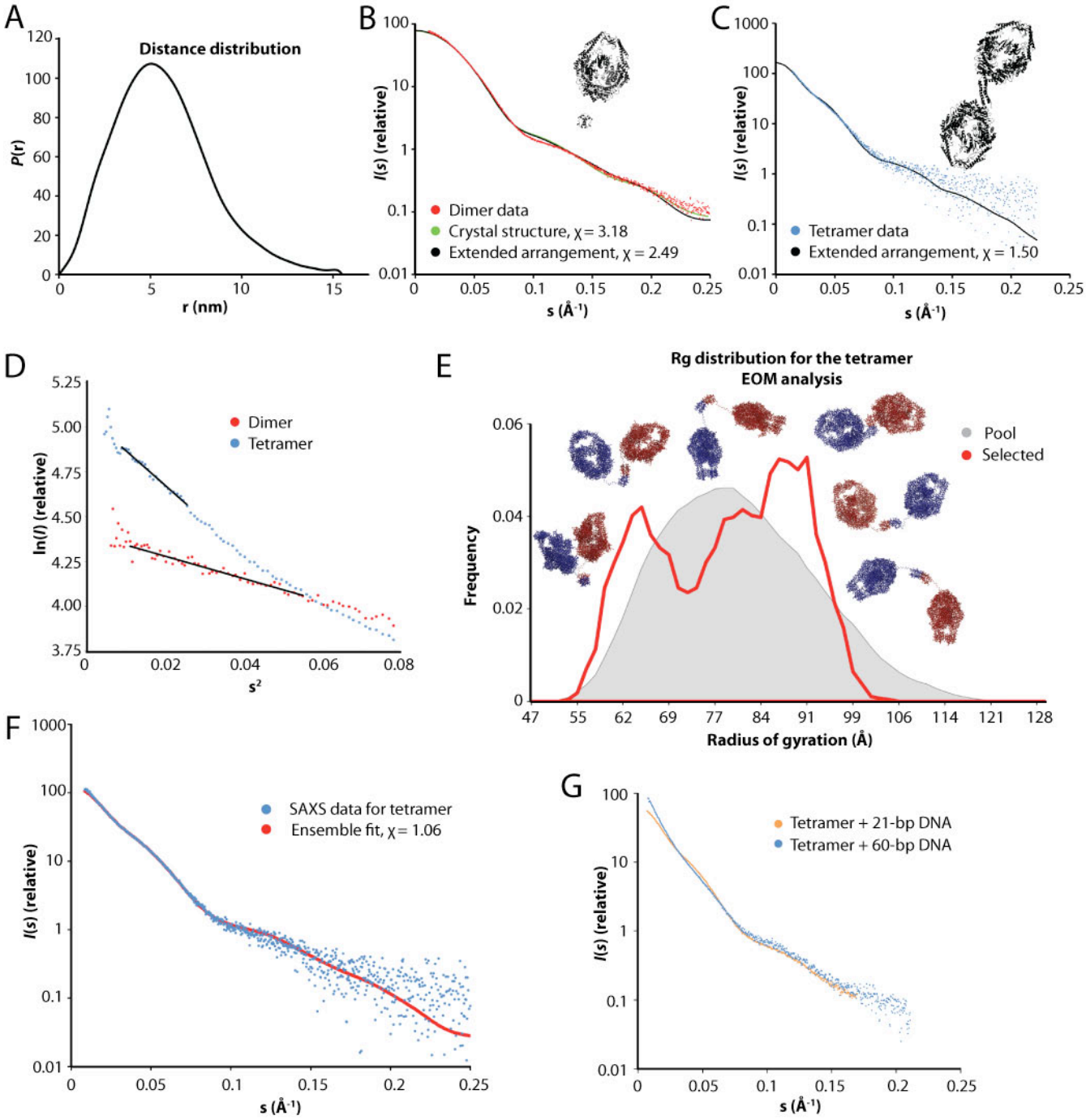


*Supplementary Figure 2.* SAXS analysis for the MutS dimer and tetramer. The scattering curves are displaced in logarithmic scale for better visualization. (A) Distance distribution plot for the SAXS data for the MutS D835R dimer mutant. (B) Predicted curves for crystal structure of MutS D835R (green) and the dimerized core of MutS and the dimerized C-terminal domains as fitted in the SAXS envelope (black) based on scattering for the MutS D835R dimer mutant (red). (C) Predicted curve (black) for two MutS cores and the tetramerized C-terminal domains as fitted in the SAXS envelope based on scattering for the cross-linked MutS tetramer (blue). (D) Guinier plots for the SAXS data of the dimer (red) and the tetramer (blue). (E) For EOM analysis of the SAXS data of the cross-linked tetramer of MutS, 10000 conformations were generated based on the crystal structure of the dimerized residues 1-800 (from our MutS D835R structure) linked flexibly by 22 dummy atoms to tetramerized C-terminal domains (derived from PDB entry 2OK2). The distribution of different conformations over $R_g$ is plotted. Gray curve: pool of generated

conformations. Red curve: selected conformations that together describe the scattering curve best. Conformations representative of the major peak from the EOM analysis are shown. (F) Fit (red line) of the EOM selected conformations to the SAXS data (blue dots). (G) SAXS data curves for the cross-linked MutS tetramer bound to 21-bp DNA (orange) and 60-bp DNA (blue).

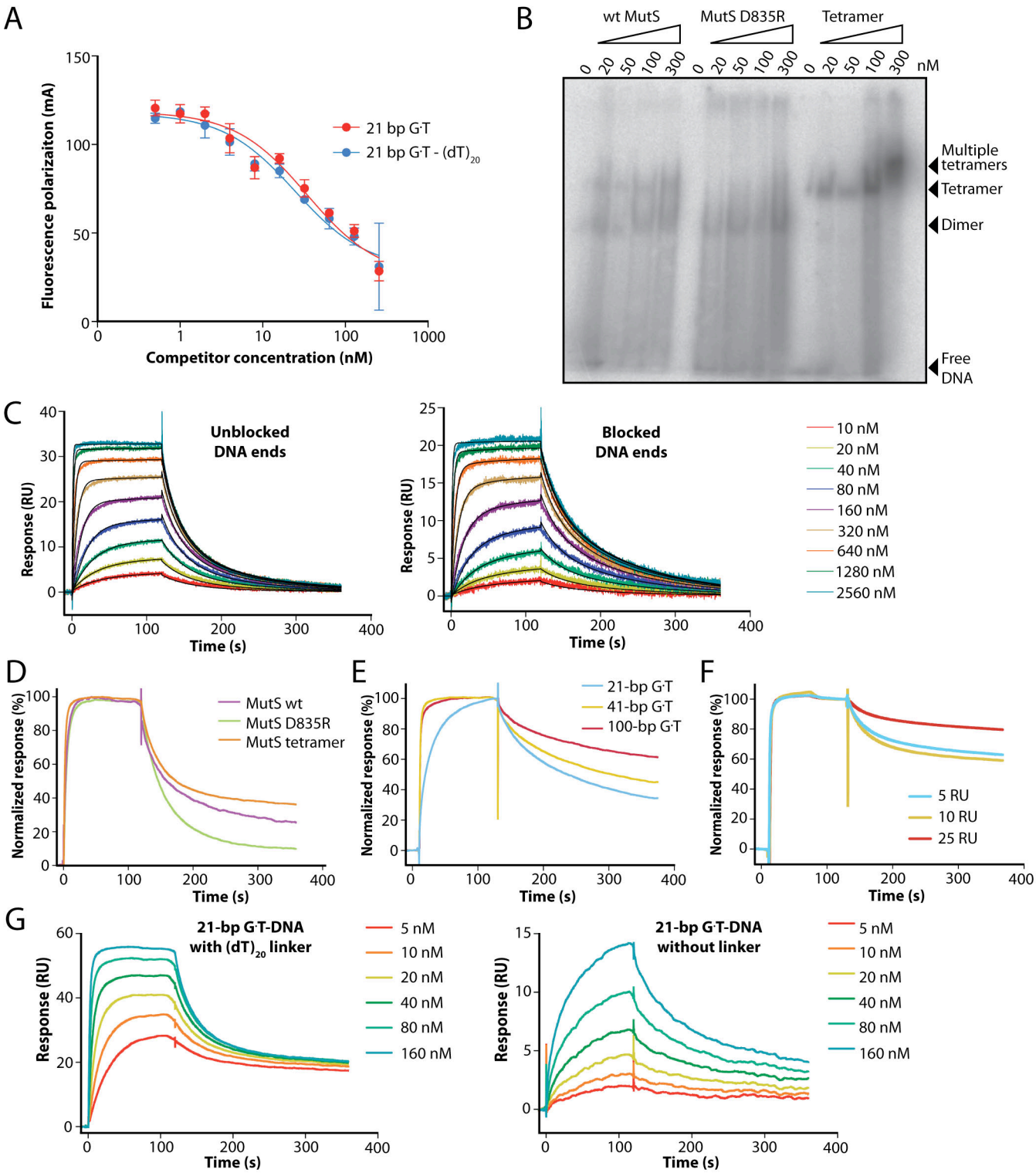


*Supplementary Figure 3.* DNA binding by the different MutS oligomers. (A) Fluorescence polarization experiment with the MutS D835R dimer. When MutS is bound to 21-bp DNA with a G·T mismatch and a 5' fluorescent TAMRA label, same-sequence 21-bp DNA can compete for binding as well as a 21-bp duplex with a $(dT)_{20}$ ssDNA overhang, suggesting no extra binding of MutS to the ssDNA. (B) An EMSA assay shows shifts of radioactively labeled 41-bp heteroduplexes of DNA due to binding of wild-type MutS, dimeric MutS D835R or cross-linked tetrameric MutS (numbers refer to monomer concentrations in nM). First and second shift correspond dimer and tetramer binding respectively, whereas the highest shift indicates multiple binding by the tetramer at high protein concentration. When using wild type MutS, shifts

corresponding to both dimer and tetramer species are observed at each protein concentration. (C) SPR experiments of the MutS D835R dimer binding to unblocked and end-blocked DNA. Multiple concentrations of protein were flown over a chip with DNA with a G·T mismatch (Supplementary Table 1). The dimer shows similar kinetic profiles in SPR measurements when binding to DNA with unblocked ends (top graph) or DNA with blocked ends (bottom graph). In both cases, kinetics can be fitted using a one-phase binding model. (D) Normalized superposition of SPR measurements of 160 nM (monomer concentrations) of wild type MutS, dimeric MutS D835R or the cross-linked MutS tetramer binding to DNA with a G·T mismatch (Supplementary Table 1). Differences in kinetics can be observed between the oligomers: tetrameric MutS (orange curve) has a slower dissociation from the DNA, while dimeric MutS D835R (green curve) comes off fast. Wild type MutS (purple curve) appears to have a profile that is an intermediate of dimer and tetramer dissociations, suggesting a combination of these two kinetic profiles. (E) Normalized SPR measurements show binding of 320 nM (monomer concentration) of the tetramer of MutS to different lengths of DNA with a G·T mismatch (21-bp, 41-bp or 100-bp) immobilized on the chip without ssDNA linker. The slow dissociation of the tetramer is more pronounced with increasing DNA length. The peak at 120 s is due to the switch to the buffer injection step. (F) Normalized SPR measurements show binding of 320 nM (monomer concentration) of the tetramer of MutS to DNA with a G·T mismatch (Supplementary Table 1) immobilized with varying amounts (5, 10 or 25 RU). Different amounts of immobilized DNA correspond to different DNA densities on the chip surface. If the stronger binding of the tetramer observed in our assays was due to binding of two DNA strands in each of its two DNA-binding sites, this effect would be greater in the case of higher DNA density. We only see an increased effect when immobilizing as much as 25 RU, but not at the ~7 RU range that was used in all standard SPR experiments. (G) SPR measurements of different concentrations of the tetramer of MutS binding to 21-bp DNA with a G·T mismatch, either directly immobilized to the chip (right graph) of via a $(dT)_{20}$ linker (left graph). In the case of no ssDNA linker, the tetramer shows continuing dissociation, indicating that the slow tetramer dissociation in the assay with ssDNA linker is not due to aggregation under the experimental conditions.

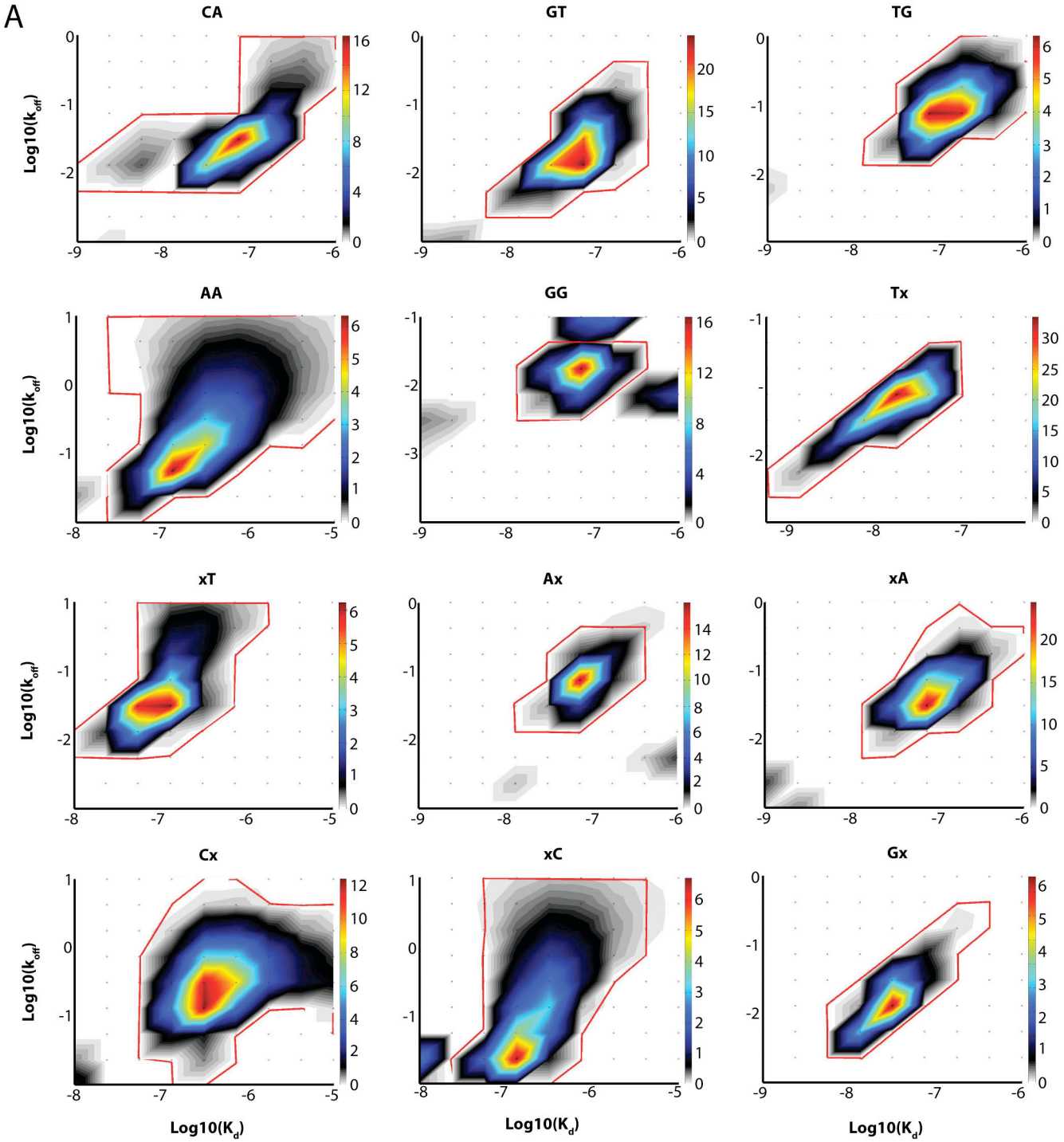
A
CA
GT
TG
AA
GG
Tx
xT
Ax
xA
Cx
xC
Gx
Log10(k_off)
Log10(K_d)

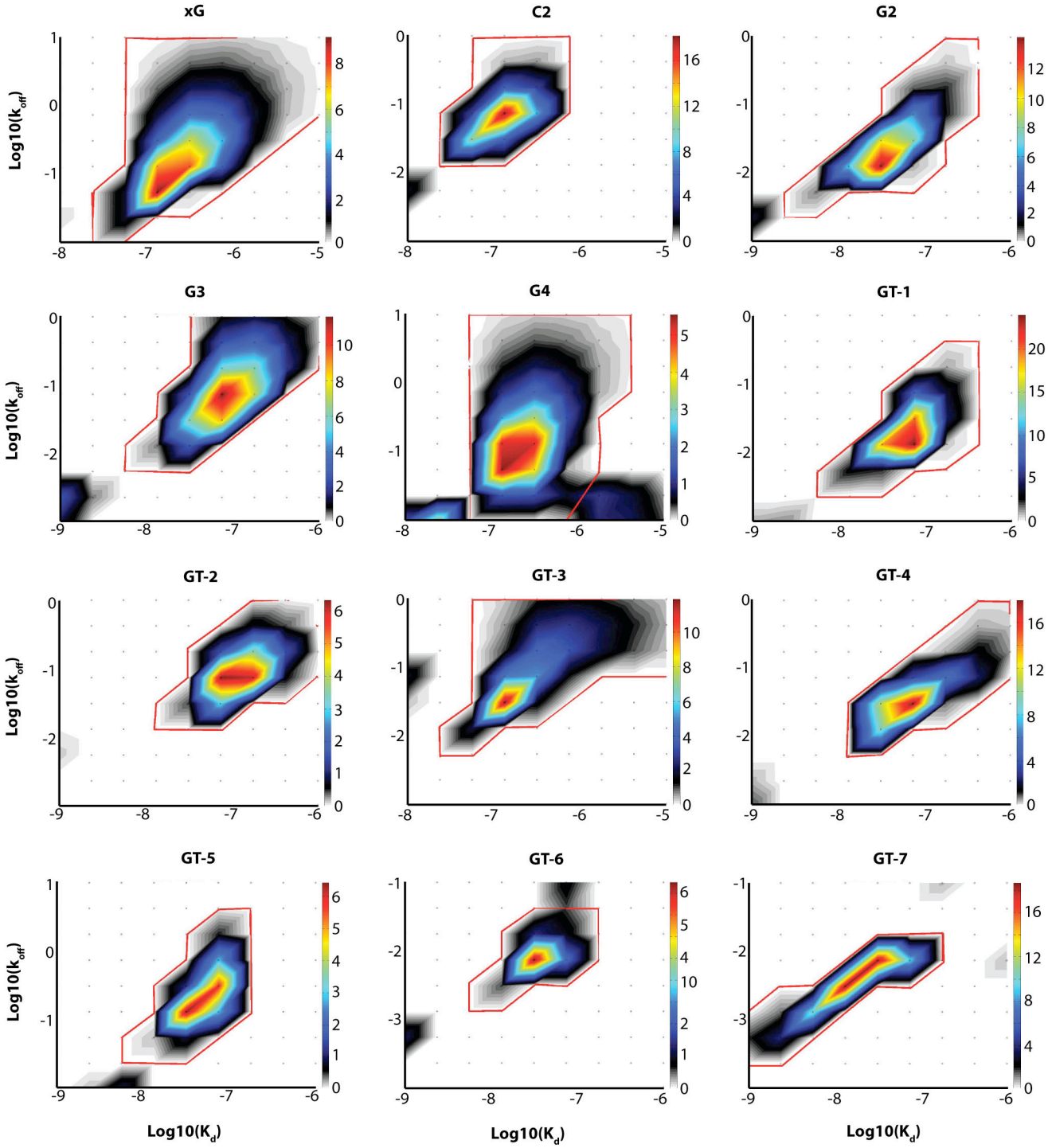
xG
C2
G2
G3
G4
GT-1
GT-2
GT-3
GT-4
GT-5
GT-6
GT-7
Log10(k_off)
Log10(K_d)

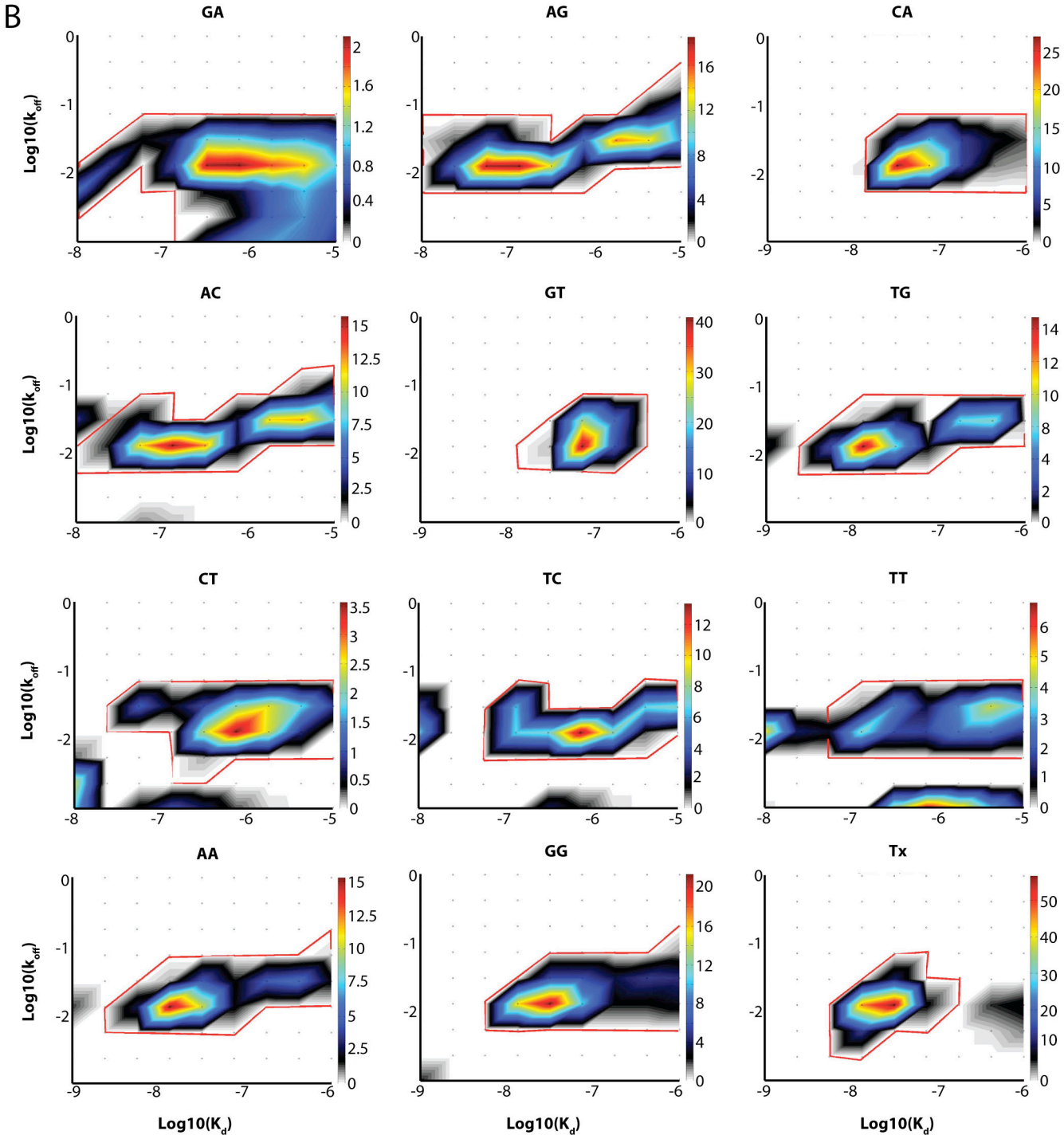
B
GA
AG
CA
AC
GT
TG
CT
TC
TT
AA
GG
Tx
Log10(k_off)
Log10(K_d)

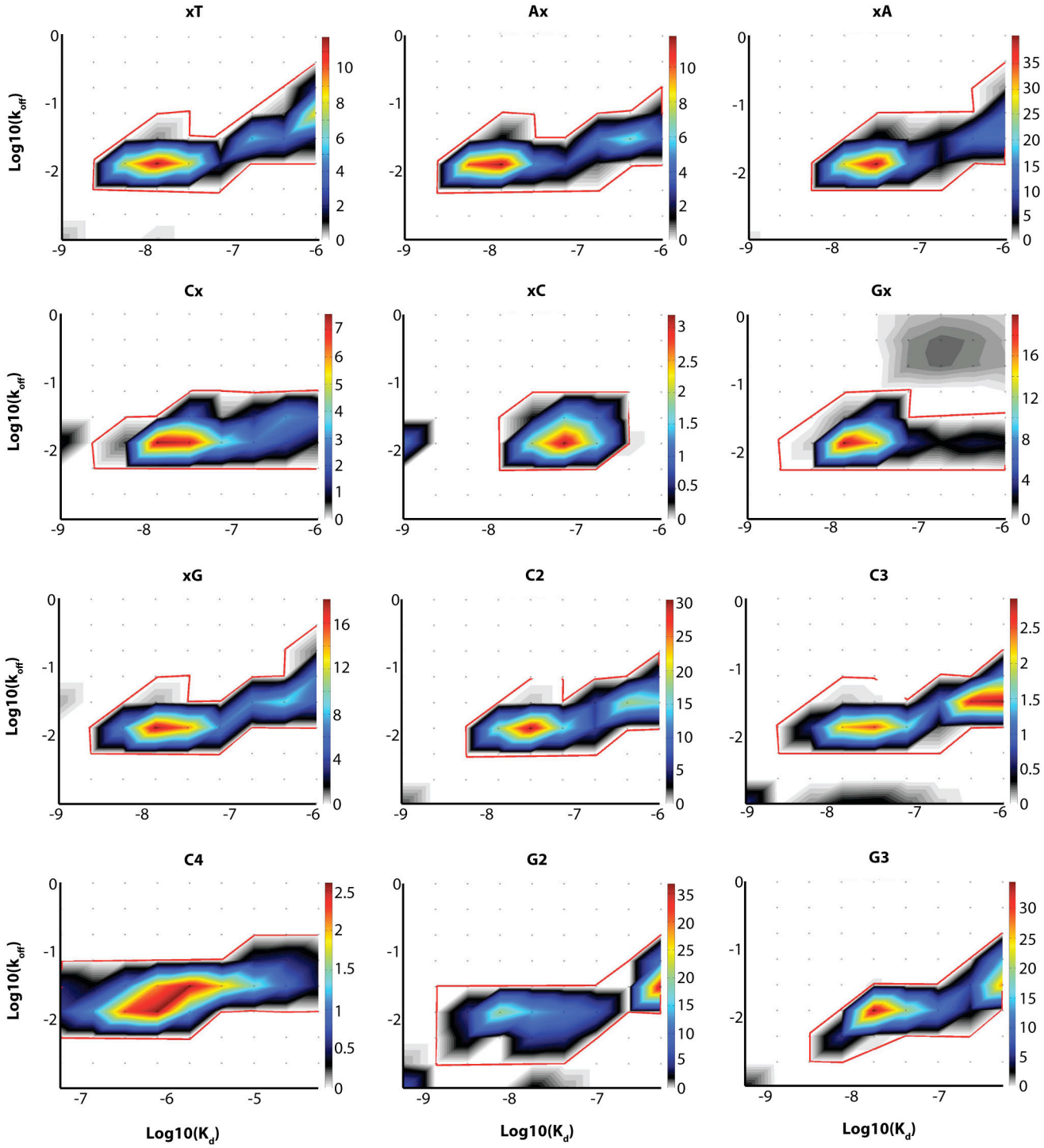
xT
Ax
xA
Cx
xC
Gx
xG
C2
C3
C4
G2
G3
Log10(k_off)
Log10(K_d)

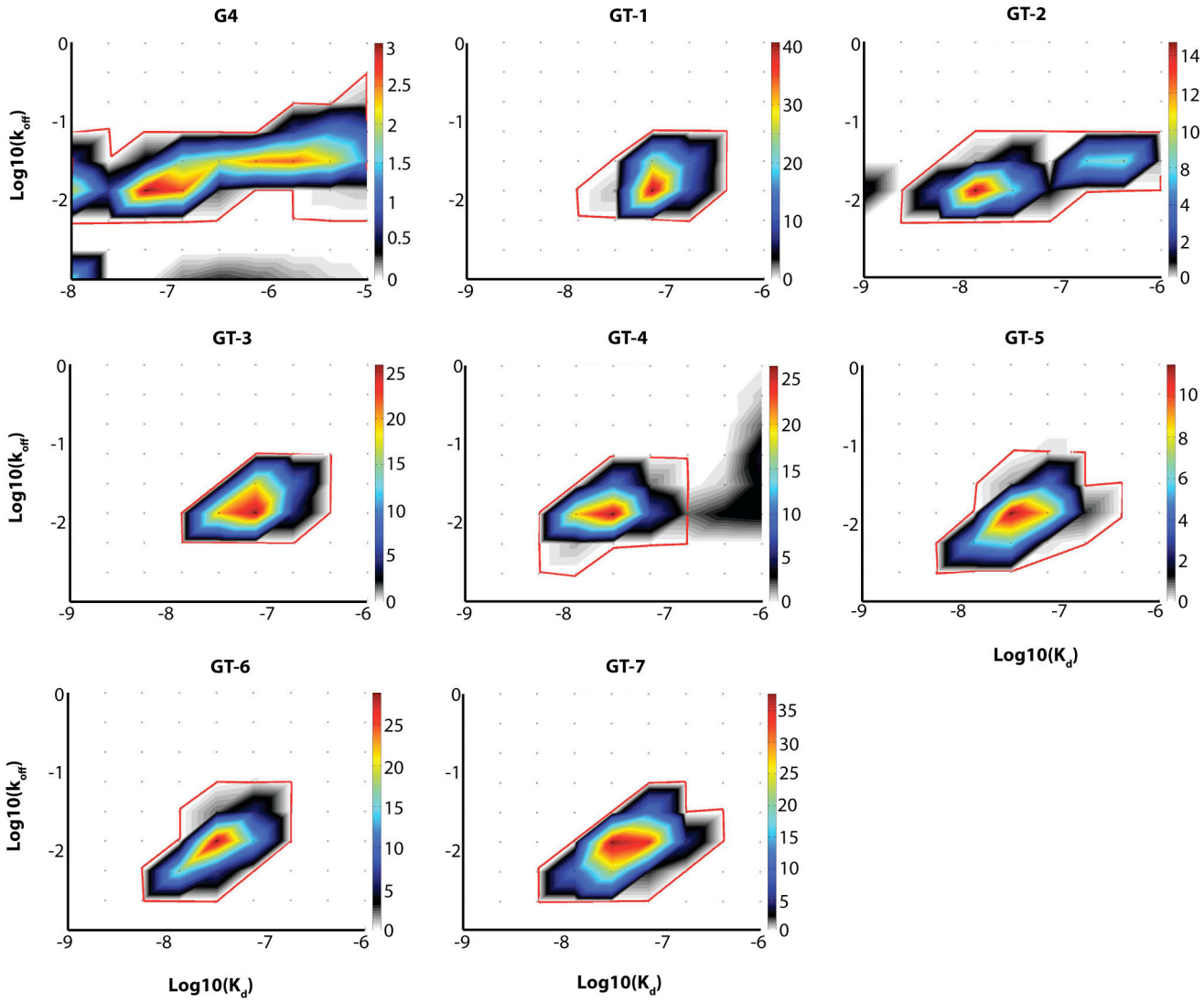


*Supplementary Figure 4.* Examples of EvilFit heat maps for determination of kinetic parameters of MutS binding. Areas for which a weighted average was taken to obtain parameters are lined in red. (A) Measurements in absence of ATP, (B) measurements in presence of 1 mM ATP.

## SUPPLEMENTARY TABLES

*Supplementary Table 1.* Sequences used in the SPR screen for binding of MutS to different mismatches. Via a biotin-label attached at the end of the $(dT)_{20}$ ssDNA linker, the DNA was immobilized on a Biacore streptavidin chip. 'Flu' indicates a fluorescein moiety coupled to the indicated strand. The asterisks indicate positions of bases that were varied. In the case of insertions larger than one base, the extra bases were placed at the position of the asterisk in the bottom strand. For G·T-1 to G·T-7, colors of the flanking sequences correspond to the schematic representation in Figure 6B.

| | |
|---|---|
| Standard DNA sequence | Flu 5′ **AGTCGCCAGG * ACCAGTGTCA** $(dT)_{20}$ 3′<br>3′ **TCAGCGGTCC * TGGTCACAGT** 5′ |
| G·T-1 | Flu 5′ AGTCGCCAGG G ACCAGTGTCA $(dT)_{20}$ 3′<br>3′ TCAGCGGTCC T TGGTCACAGT 5′ |
| G·T-2 | Flu 5′ AGTCGCCAGG T ACCAGTGTCA $(dT)_{20}$ 3′<br>3′ TCAGCGGTCC G TGGTCACAGT 5′ |
| G·T-3 | Flu 5′ TCAGCGGTCC G ACCAGTGTCA $(dT)_{20}$ 3′<br>3′ AGTCGCCAGG T TGGTCACAGT 5′ |
| G·T-4 | Flu 5′ TCAGCGGTCC T ACCAGTGTCA $(dT)_{20}$ 3′<br>3′ AGTCGCCAGG G TGGTCACAGT 5′ |
| G·T-5 | 5' TCAGCGGTCC G TGGTCACAGT 3'<br>Flu 3' AGTCGCCAGG T ACCAGTGTCA $(dT)_{20}$ 5′ |
| G·T-6 | 5' TCAGCGGTCC T TGGTCACAGT 3'<br>Flu 3' AGTCGCCAGG G ACCAGTGTCA $(dT)_{20}$ 5′ |
| G·T-7 | 5' AGTCGCCAGG T TGGTCACAGT 3'<br>Flu 3' TCAGCGGTCC G ACCAGTGTCA $(dT)_{20}$ 5′ |

*Supplementary Table 2.* Activities of MutS variants *in vivo* and *in vitro*.

| Variant[a] | *In vivo* | | *In vitro*[d] | |
|---|---|---|---|---|
| | Median[b] | Range[c] | Relative activity (%) | S.D. (%) |
| pET-15b vector | 230 | 142-250 | - | - |
| wild-type MutS | 2 | 0-15 | 100 | 1 |
| cysteine-free MutS | 3 | 1-11 | 98 | 7 |
| single-cysteine MutS R848C | 10 | 1-59 | 113 | 3 |

[a] *E. coli* TX2929 (*mutS*⁻) was transformed with the plasmid pET-15b (vector control), wild type *mutS* or *mutS* mutants as indicated. For details see Supplementary Materials and Methods.
[b] Median number of rifampicin-resitant clones as counted on individual plates, which arise by spontaneous mutation in the *rpoB* gene. Cells lacking a functional MutS protein have a higher frequency of mutation.
[c] Minimum and maximum number of rifampicin-resitant clones on individual plates.
[d] DNA cleavage by MutS-activated MutH. 400 nM MutS, 1 μM MutL and 200 nM MutH were used to cleave 10 nM 484-bp G·T mismatch containing DNA.

## SUPPLEMENTARY REFERENCES


60. Loh,T., Murphy,K.C. and Marinus,M.G. (2001) Mutational Analysis of the MutH Protein from *Escherichia coli*. *J. Biol. Chem.*, **276**, 12113–12119.

61. Feng,G. and Winkler,M.E. (1995) Single-step purifications of His6-MutH, His6-MutL and His6-MutS repair proteins of escherichia coli K-12. *BioTechniques*, **6**, 956–965.

62. Xiao,Y., Jung,C., Marx,A.D., Winkler,I., Wyman,C., Lebbink,J.H.G., Friedhoff,P. and Cristovao,M. (2011) Generation of DNA nanocircles containing mismatched bases. *BioTechniques*, **51**, 259–265.